Acta Crystallographica Section F
Structural Biology and Crystallization Communications
ISSN 1744-3091

Crystallization and preliminary crystallographic analysis of the ferredoxin component of carbazole 1,9a-dioxygenase from *Nocardioides aromaticivorans* IC177

Kengo Inoue,[a] Yuji Ashikawa,[a]‡ Yusuke Usami,[a] Haruko Noguchi,[a,b] Zui Fujimoto,[c] Hisakazu Yamane[a] and Hideaki Nojiri[a,b]*

[a]Biotechnology Research Center, The University of Tokyo, 1-1-1 Yayoi, Bunkyo-ku, Tokyo 113-8657, Japan, [b]Professional Programme for Agricultural Bioinformatics, The University of Tokyo, 1-1-1 Yayoi, Bunkyo-ku, Tokyo 113-8657, Japan, and [c]Protein Research Unit, National Institute of Agrobiological Sciences, 2-1-2 Kannondai, Tsukuba, Ibaraki 305-8602, Japan

‡ Present address: Molecular Signaling Research Team, Structural Physiology Research Group, RIKEN Spring-8 Center, Harima Institute, 1-1-1 Kouto, Sayo, Hyogo 679-5148, Japan.

Correspondence e-mail: anojiri@mail.ecc.u-tokyo.ac.jp

Received 9 July 2007
Accepted 22 August 2007

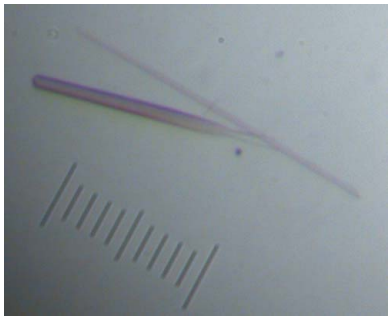

Carbazole 1,9a-dioxygenase (CARDO) catalyzes the dihydroxylation of carbazole by angular position (C9a) carbon bonding to the imino nitrogen and its adjacent C1 carbon. CARDO consists of a terminal oxygenase component and two electron-transfer components: ferredoxin and ferredoxin reductase. The ferredoxin component of carbazole 1,9a-dioxygenase from *Nocardioides aromaticivorans* IC177 was crystallized at 293 K using the hanging-drop vapour-diffusion method with ammonium sulfate as the precipitant. The crystals, which were improved by macroseeding, diffract to 2.0 Å resolution and belong to space group $P4_12_12$.

1. Introduction

Rieske nonhaem iron oxygenase systems (ROSs) are the initial catalysts in the degradation pathways of various environmentally important aromatic compounds, including dioxins, polychlorinated biphenyls and crude-oil components such as polycyclic aromatic hydrocarbons and carbazole (Wittich, 1998; Bressler & Fedorak, 2000; Nojiri & Omori, 2002; Habe & Omori, 2003; Furukawa *et al.*, 2004). The ROSs typically consist of two or three components that comprise an electron-transfer chain, mobilizing electrons from NADH or NADPH *via* flavin and [2Fe–2S] redox centres to the site of dioxygen activation. The ROSs have been classified into five groups, IA, IB, IIA, IIB and III, based on their number of constituents and the nature of their redox centres (Batie *et al.*, 1991). The three-component systems consisting of terminal oxygenase, ferredoxin and ferredoxin reductase components have been classified into classes IIA, IIB or III. The class IIB and III ROSs commonly have a Rieske-type ferredoxin. However, the class IIB and III ROSs have a ferredoxin reductase component that contains only FAD, and contains FAD and a chloroplast-type [2Fe–2S] cluster, respectively.

The Gram-positive carbazole degrader *Nocardioides aromaticivorans* IC177 possesses a carbazole 1,9a-dioxygenase (CARDO; Fig. 1; Inoue *et al.*, 2005; Inoue, Habe *et al.*, 2006). CARDO consists of three components: the terminal oxygenase CARDO-O, the ferredoxin CARDO-F and the ferredoxin reductase CARDO-R, which are encoded by the *carAa*, *carAc* and *carAd* genes, respectively. The CARDO of *N. aromaticivorans* IC177 is classified as a class IIB ROS (Inoue, Habe *et al.*, 2006), while the well studied CARDOs from *Pseudomonas resinovorans* CA10, *Janthinobacterium* sp. J3 and *Sphingomonas* sp. KA1 are classified into classes III, III and IIA, respectively (Sato *et al.*, 1997; Inoue *et al.*, 2004; Urata *et al.*, 2006). CARDOs have diverse types of electron-transfer components (*e.g.* CARDO-F and CARDO-R) and a high similarity (>45% identity at the amino-acid sequence level) within the terminal oxygenase. Although the structures of several ROS proteins are known (Ferraro *et al.*, 2005), the precise nature of the electron-transfer mechanism remains to be determined. Therefore, CARDO is an excellent model system for studying structure–function relationships of ROS-like enzymes and the mechanism of electron transfer.

We have determined the structures of CARDO-O of *Janthinobacterium* sp. J3 (Nojiri *et al.*, 2005), CARDO-F of *P. resinovorans* CA10 (Nam *et al.*, 2005) and the complex of CARDO-O of *Janthinobacterium* sp. J3 with CARDO-F of *P. resinovorans* CA10

(Ashikawa *et al.*, 2005, 2006). The structure of the complex of CARDO-O of *Janthinobacterium* sp. J3 with CARDO-F of *P. resinovorans* CA10 revealed interacting sites in the respective components (Ashikawa *et al.*, 2006). Using these results and also determining the structure of CARDO-O of *N. aromaticivorans* IC177 (Inoue, Ashikawa *et al.*, 2006; unpublished data), we identified several amino acids that may be crucial in CARDO protein–protein interactions. Structural analyses of the molecular surface of CARDO-F of *P. resinovorans* CA10 and *N. aromaticivorans* IC177 will provide more detailed information about the protein–protein interaction that is necessary for electron transfer in ROSs.

In phylogenetic analyses, the CARDO-O of *N. aromaticivorans* IC177 appears to be closely related to homologous proteins from *P. resinovorans* CA10 and *Janthinobacterium* sp. J3, although the CARDO-F of *N. aromaticivorans* IC177 does not have very close phylogenetic relationships with CARDO-F from *P. resinovorans* CA10 and *Janthinobacterium* sp. J3 (Inoue, Habe *et al.*, 2006). However, interestingly, the CARDO-F of *N. aromaticivorans* IC177 is also not very closely related to the ferredoxin components of typical class IIB ROSs, such as biphenyl dioxygenases and toluene dioxygenases (Inoue, Habe *et al.*, 2006), implying that the CARDO-F of *N. aromaticivorans* IC177 has a unique evolutionary origin.

In this report, we describe the crystallization of and preliminary X-ray diffraction studies on the CARDO-F of *N. aromaticivorans* IC177 (composed of 115 amino acids with an amino-acid-based molecular weight of 12.3 kDa).

2. Protein expression and purification

The *carAc* gene (accession No. BAE79502) was amplified by PCR from plasmid pB177106 (Inoue, Habe *et al.*, 2006) using primers 5′-TCTAGAGTAAGGAGGTGTTCATATGAACAGGCATTCGGCGGG-3′ and 5′-ACTAGTAAGCTTTCA**GTGGTGGTGGTGGTGGTG**TCTGCCTCCTTCGGCGCCA-3′ (the sequence for the His tag is indicated in bold). The PCR product was ligated into the pT7Blue T vector (Novagen). The nucleotide sequence of the insert was checked against the original sequence and the plasmid was digested with *Nde*I and *Hin*dIII. A 0.4 kbp *Nde*I–*Hin*dIII fragment was inserted into the overexpression vector pET-26b(+) (Novagen; designated pE177506). pE177506 contains the genes for the full-length CARDO-F with a 6×His tag in the C-terminal region (ht-CARDO-F). Transformed *Escherichia coli* BL21 (DE3) (Novagen) cells were grown at 298 K on SB medium (Nam *et al.*, 2002) supplemented with 0.5 m*M* IPTG. After a 15 h incubation, the cells were harvested by centrifugation at 5000*g* for 10 min, washed twice with TG buffer (Nam *et al.*, 2002) and resuspended in buffer *A* (20 m*M* Tris–HCl pH 7.5 containing 0.5 *M* NaCl and 10% glycerol). The crude cell extract was prepared by sonication and centrifugation at 25 000*g* for 2 h and was applied onto a HiTrap Chelating HP column (GE Healthcare) equipped with an ÄKTA FPLC instrument (GE Healthcare) according to the manufacturer's recommendations. ht-CARDO-F was eluted with buffer *B* (buffer *A* containing 300 m*M* imidazole). The fractions containing ht-CARDO-F were pooled and concentrated by ultrafiltration using Centriprep YM-10 (Millipore). The resultant preparation was further purified by gel-filtration chromatography using a Superdex 200 prep-grade (GE Healthcare) column and GFC buffer (Nam *et al.*, 2002). During purification using gel-filtration chromatography, the putative ht-CARDO-F eluted at a position corresponding to a protein of molecular weight $\simeq$ 5.5 kDa, although SDS–PAGE confirmed the theoretical molecular weight of ht-CARDO-F as ∼13 kDa (data not shown). The precise molecular weight of ht-CARDO-F was measured by matrix-assisted laser desorption ionization time-of-flight mass spectrometry (MALDI–TOF MS; Voyager-DE STR, Applied Biosystems). A saturated supernatant of sinapinic acid in 60% acetonitrile and 0.1% trifluoroacetic acid was prepared as a matrix solution. A mixture of the matrix solution and 1–5 pmol ht-CARDO-F was analyzed in a positive linear mode at an accelerating voltage of 20 kV. The mass spectrum of ht-CARDO-F showed an ion peak at *m*/*z* 13 148, which corresponds to the theoretical single methionine-oxidized molecular weight of 13 145 Da. Before crystallization, the purified ht-CARDO-F was confirmed to retain its reduction activity for the terminal oxygenase CARDO-O from *N. aromaticivorans* IC177 when coupled with the electron-transfer protein CARDO-R from *N. aromaticivorans* IC177 and NADH and monitored by UV and visible absorption measurements (data not shown). These data indicated that CARDO-F from *N. aromaticivorans* IC177 is active as a monomer similar in nature to that of CARDO-F from *P. resinovorans* CA10 (Nam *et al.*, 2002). Protein concentrations were estimated using a protein-assay kit (Bio-Rad; Bradford, 1976) with BSA as a standard. For crystallization experiments, a solution of the protein in 5 m*M* Tris–HCl pH 7.5 with a CARDO-F concentration in the range 5–30 mg ml^{-1} was used.

3. Crystallization

Crystallization was performed using the hanging-drop vapour-diffusion method at 293 and 278 K. Drops containing 2 µl protein solution and 2 µl mother liquor were equilibrated against 800 µl

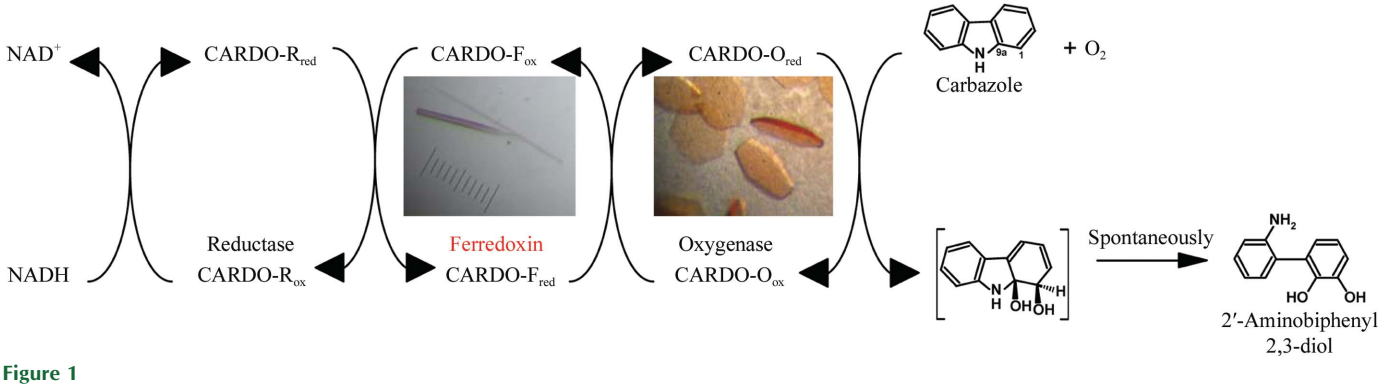

Figure 1
Components and functions of the CARDO system. The proposed electron-transfer reactions and the conversion of carbazole to 2′-aminobiphenyl-2,3-diol are illustrated. The subscripts 'ox' and 'red' indicate the oxidized and reduced states of the CARDO components, respectively. The CARDO-F (this study) and CARDO-O (Inoue, Ashikawa *et al.*, 2006) crystals are shown.

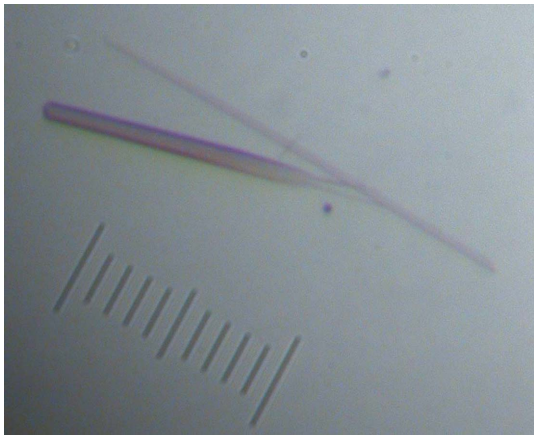

Figure 2
Crystals of CARDO-F from *N. aromaticivorans* IC177. The scale bar indicates 0.16 mm.

reservoir solution. An initial screen was performed using Crystal Screens I and II, Crystal Screen Cryo, Salt RX, Grid Screen Ammonium Sulfate, Grid Screen Sodium Malonate and Index Screen (Hampton Research). Several crystals were obtained using Crystal Screen II condition No. 14 (0.1 *M* trisodium citrate dehydrate pH 5.6, 2.0 *M* ammonium sulfate and 0.2 *M* potassium sodium tartrate tetrahydrate) in the reservoir and protein solution with a concentration of 20 mg ml^{-1}. Reddish needle-shaped crystals appeared within 3 d. To improve their quality, they were subjected to macroseeding using drops containing 2.0, 1.5, 1.0 or 0.5 µl protein solution (1–60 mg ml^{-1}) and 2 µl mother liquor. The final crystals, which grew to typical dimensions of 15 × 15 × 200 µm (Fig. 2), were obtained by macroseeding at 293 K with drops containing 0.5 µl protein solution (2 mg ml^{-1}) and 2 µl mother liquor.

4. X-ray analysis

Diffraction experiments were conducted using a Quantum (Q4R) area detector (Area Detector Systems Corp.) on beamline BL-17A at Photon Factory (Tsukuba, Japan). The crystals were transferred directly into a cryoprotectant solution containing 8% glycerol and 92% crystallization solution and flash-cooled in a nitrogen stream at 100 K. A total range of 115° was covered with 1.0° oscillation at λ = 1.0 Å. The diffraction data were processed and scaled using the *HKL*-2000 program suite (Otwinowski & Minor, 1997). A data set was collected to 2.0 Å resolution. The data-collection and processing statistics are summarized in Table 1. The space group of the crystal was determined to be $P4_12_12$ or $P4_32_12$, with unit-cell parameters $a = b = 50.12$, $c = 82.22$ Å. Initial analyses of the crystal solvent content using the Matthews coefficient (Matthews, 1968) suggested that the asymmetric unit contains one protein molecule (37.4% solvent content), with an acceptable packing density V_M of 1.97 Å^3 Da^{-1}. The crystal structure solution was attempted using the molecular-replacement method with the structure of ht-CARDO-F from *P. resinovorans* CA10 (31% amino-acid sequence identity; Nam *et al.*, 2005) as a search model. As a result, the space group was ultimately determined to be $P4_12_12$. A full description of the structure determination will be published elsewhere.

Table 1
Crystal parameters and data-collection statistics.

The data were collected on BL-17A at Photon Factory, Tsukuba, Japan. Values in parentheses are for the highest resolution shell.

Wavelength (Å)	1.0
Space group	$P4_12_12$
Unit-cell parameters (Å)	$a = b = 50.12$, $c = 82.22$
Resolution range (Å)	50.0–2.0 (2.06–2.0)
Total no. of reflections	66413
No. of unique reflections	7802 (738)
Completeness (%)	99.8 (97.6)
Average $I/\sigma(I)$	39.7 (9.0)
R_{merge}† (%)	8.6 (29.9)
Multiplicity	8.5 (8.2)

† $R_{merge} = \sum_{\mathbf{h}} \sum_l |I_{\mathbf{h}l} - \langle I_{\mathbf{h}} \rangle| / \sum_{\mathbf{h}} \sum_l \langle I_{\mathbf{h}} \rangle$, where $I_{\mathbf{h}l}$ is the lth observation of reflection **h** and $\langle I_{\mathbf{h}l} \rangle$ is the weighted average intensity for all observations l of reflection **h**.

We thank Dr S. Nagata of the University of Tokyo for MALDI–TOF MS analysis. This study was partly supported by a Grant-in-Aid for Scientific Research (17380052; to HN) from the Ministry of Education, Culture, Sports, Science and Technology, Japan. KI was supported by the Japan Society for the Promotion of Science for Young Scientists. The use of synchrotron radiation for this work was approved by the Photon Factory Advisory Committee and KEK (High Energy Accelerator Research Organization), Tsukuba, Japan (proposal Nos. 2005G060 and 2006G171).

References

Ashikawa, Y., Fujimoto, Z., Noguchi, H., Habe, H., Omori, T., Yamane, H. & Nojiri, H. (2005). *Acta Cryst.* F**61**, 577–580.
Ashikawa, Y., Fujimoto, Z., Noguchi, H., Habe, H., Omori, T., Yamane, H. & Nojiri, H. (2006). *Structure*, **14**, 1779–1789.
Batie, C. J., Ballou, D. P. & Correll, C. C. (1991). *Chemistry and Biochemistry of Flavoenzymes*, Vol. 3, edited by F. Muller, pp. 543–556. Boca Raton: CRC Press.
Bradford, M. M. (1976). *Anal. Biochem.* **72**, 248–254.
Bressler, D. C. & Fedorak, P. M. (2000). *Can. J. Microbiol.* **46**, 397–409.
Ferraro, D. J., Gakhar, L. & Ramaswamy, S. (2005). *Biochem. Biophys. Res. Commun.* **338**, 175–190.
Furukawa, K., Suenaga, H. & Goto, M. (2004). *J. Bacteriol.* **186**, 5189–5196.
Habe, H. & Omori, T. (2003). *Biosci. Biotechnol. Biochem.* **67**, 225–243.
Inoue, K., Ashikawa, Y., Usami, Y., Noguchi, H., Fujimoto, Z., Yamane, H. & Nojiri, H. (2006). *Acta Cryst.* F**62**, 1212–1214.
Inoue, K., Habe, H., Yamane, H. & Nojiri, H. (2006). *Appl. Environ. Microbiol.* **72**, 3321–3329.
Inoue, K., Habe, H., Yamane, H., Omori, T. & Nojiri, H. (2005). *FEMS Microbiol. Lett.* **245**, 145–153.
Inoue, K., Widada, J., Nakai, S., Endoh, T., Urata, M., Ashikawa, Y., Shintani, M., Saiki, Y., Yoshida, T., Habe, H., Omori, T. & Nojiri, H. (2004). *Biosci. Biotechnol. Biochem.* **68**, 1467–1480.
Matthews, B. W. (1968). *J. Mol. Biol.* **33**, 491–497.
Nam, J.-W., Noguchi, H., Fujimoto, Z., Mizuno, H., Ashikawa, Y., Abo, M., Fushinobu, S., Kobashi, K., Wakagi, T., Iwata, K., Yoshida, T., Habe, H., Yamane, H., Omori, T. & Nojiri, H. (2005). *Proteins*, **58**, 779–789.
Nam, J.-W., Nojiri, H., Noguchi, H., Uchimura, H., Yoshida, T., Habe, H., Yamane, H. & Omori, T. (2002). *Appl. Environ. Microbiol.* **68**, 5882–5890.
Nojiri, H., Ashikawa, Y., Noguchi, H., Nam, J.-W., Urata, M., Fujimoto, Z., Yoshida, T., Habe, H. & Omori T. (2005). *J. Mol. Biol.* **351**, 355–370.
Nojiri, H. & Omori, T. (2002). *Biosci. Biotechnol. Biochem.* **66**, 2001–2016.
Otwinowski, Z. & Minor, W. (1997). *Methods Enzymol.* **276**, 307–326.
Sato, S., Nam, J.-W., Kasuga, K., Nojiri, H., Yamane, H. & Omori, T. (1997). *J. Bacteriol.* **179**, 4850–4858.
Urata, M., Uchimura, H., Noguchi, H., Sakaguchi, T., Takemura, T., Eto, K., Habe, H., Omori, T., Yamane, H. & Nojiri, H. (2006). *Appl. Environ. Microbiol.* **72**, 3206–3216.
Wittich, R.-M. (1998). *Appl. Microbiol. Biotechnol.* **49**, 489–499.